Exploring the Utility of Many-Body Expansions: A Consistent Set of Accurate Potentials for the Lowest Quartet and Doublet States of the Azide Radical With Revisited Dynamics.

ARTICLE *in* THE JOURNAL OF PHYSICAL CHEMISTRY A · SEPTEMBER 2014

Impact Factor: 2.69 · DOI: 10.1021/jp5087027 · Source: PubMed

2 AUTHORS:

Antonio J. C. Varandas
University of Coimbra
382 PUBLICATIONS **6,750** CITATIONS
SEE PROFILE

Breno Galvão
Centro Federal de Educação Tecnológica de M…
16 PUBLICATIONS **73** CITATIONS
SEE PROFILE

THE JOURNAL OF PHYSICAL CHEMISTRY A

Article

pubs.acs.org/JPCA

Exploring the Utility of Many-Body Expansions: A Consistent Set of Accurate Potentials for the Lowest Quartet and Doublet States of the Azide Radical with Revisited Dynamics

A. J. C. Varandas*,† and B. R. L. Galvão*,‡

†Departamento de Química, Universidade de Coimbra, 3004-535 Coimbra, Portugal

‡Departamento de Química, Centro Federal de Educação Tecnológica de Minas Gerais, CEFET-MG, Av. Amazonas 5253, 30421-169 Belo Horizonte, Minas Gerais, Brazil

Supporting Information

ABSTRACT: Starting from reliable double many-body expansion potentials calibrated with energies calculated at the state-of-the-art ab initio level but of varying accuracies, it is shown that a single scaling parameter suffices to bring them into consistency while mimicking key experimental data and leaving mostly unaffected crossing seams of the conical type. This emerges as a valuable asset of their underlying formalism. Use of the novel potentials for studying the dynamics of the $N(^4S/^2D) + N_2(^1\Sigma_g^+)$ reactions yields results in excellent agreement with the most accurate available data.

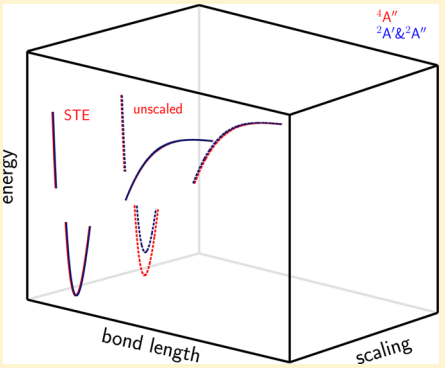

INTRODUCTION

The prediction of accurate dynamics and kinetics attributes demands an enormous effort, with the calculation of the potential energy surface(s) (PESs) being often the bottleneck. Progress in obtaining accurate ab-initio-based energies with the least computational effort has been enormous, notably via extrapolation to the complete basis set (CBS) limit[1,2] and scaling of the electron correlation.[3−6] For excited states, the problem gains enhanced complexity because multisheeted PESs are often required. In this work, it is shown how to take advantage of the many-body expansion (MBE)[7−9] formalism to bring an ab-initio-based PES (or a set of them) to experimental accuracy and obtain consistency between different levels of theories.

To illustrate the method, we consider N_3. Although being the smallest polynitrogen molecule, this intriguing species has both linear and cyclic equilibrium structures of remarkably distinct chemical characteristics and hence is challenging. While the linear N_3 is well-known experimentally,[10−14] its ring form has only recently[15−20] been detected. The PESs for ground-doublet N_3 (see Figure 1) can also be paradigmatic from the topological point of view by showing various conical intersections, including one of D_{3h} symmetry as in ground-state H_3, the long-standing workhorse of theoretical chemists[21−23] (and references therein).

Recently, we reported a set of forms that reliably describe the five PESs illustrated in Figure 1, all of the double many-body expansion (DMBE[22−26]) type and calibrated from state-of-the-art ab initio calculations.[27−29] Suffice it to say that the doublet ones[28,29] consist of two double-sheeted PESs based on MRCI(Q)/AVTZ (multireference configuration interaction energies at the aug-cc-pVTZ (AVTZ) basis set level). The quartet[27] is single-sheeted and calibrated with CBS data obtained from CCSD(T) (coupled cluster singles and doubles

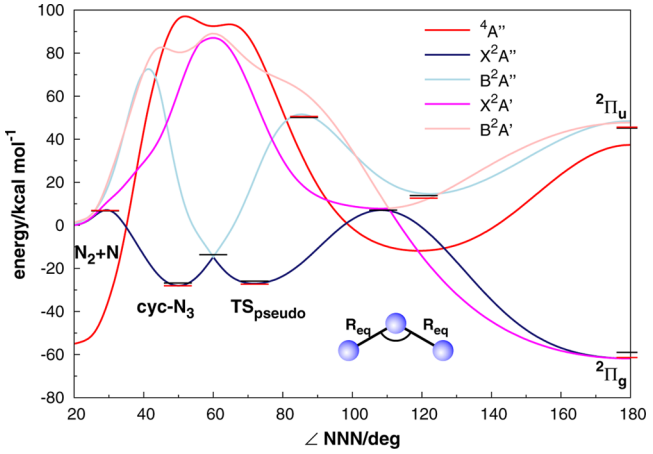

Figure 1. C_{2v} profiles with a relaxed bond length for each of the DMBE-STE PESs of N_3. The bars indicate stationary structures: black, MRCI(Q)/AVTZ; red, CBS.

Received: August 28, 2014
Revised: September 26, 2014
Published: September 26, 2014

   dx.doi.org/10.1021/jp5087027 | J. Phys. Chem. A 2014, 118, 10127−10133

with perturbative correction of triples) and MRCI(Q) raw energies, which required a smooth merging of the two distinct correlation energies via correlation scaling[30,31] (CS).

The major doublet-state structures appear well described[28] at the MRCI(Q)/AVTZ level, and hence, CBS extrapolations were deemed unnecessary for obtaining accurate $N(^2D) + N_2 \rightarrow N(^4S) + N_2$ rate constants.[32] Indeed, two-state calculations are very time-consuming at a higher level of theory. However, such a basis underestimates the well depth of N_2 by as much as 10 kcal mol^{-1}, and hence, the $N + N_2 \rightarrow 3N$ limit is not consistently described by our reported quartet and doublet PESs. It is shown here how to recalibrate all PESs to reproduce the exact atom−diatom dissociation limits because this is key for accurate reaction dynamics,[33] particularly for the calculation of dissociation rates over the whole vibrational range of N_2, which are critical for obtaining important rates of use in plasma chemistry and plasma physics[34,35] as well as re-entry problems.[36] In fact, the underlying MBE nature of the potentials allows such a recalibration to be done in a simple way without extra computational effort while preserving the reliability of the orginal fits. Due to their importance, the dynamics studies of the $N(^4S/^2D) + N_2(^1\Sigma_g^+)$ reactions will then be revisited as they also allow an accuracy check by comparing with previous results.[32,37,38]

METHOD

The MBE of a single-sheeted PES assumes the well-known form

$$V(\mathbf{R}) = V^{(1)} + \sum_{i=1}^{3} V^{(2)}(R_i) + V^{(3)}(\mathbf{R}) \tag{1}$$

where $\mathbf{R} = \{R_1,R_2,R_3\}$ is the vector of the full set of internuclear coordinates and the upper indices indicate one-body, two-body, and so on terms. In DMBE,[22−26] the cluster development in eq 1 still applies but with all terms after two-body split into two, an extended-Hartree−Fock (EHF or short-range) contribution and the dynamical correlation (dc, also known as external or long-range). Although all parameters in the EHF and dc terms could be fitted to the ab initio energies (jointly or separately), it is common practice in DMBE to fit only the EHF term to the difference between the total ab initio energy and the dc term, with this taken as a damped multipolar expansion obtained from calculated electric moments and polarizabilities of the fragments. In the following, we ignore the double partition and hence consider it as a MBE.

Denoting the four doublet PESs as V_D and the quartet as V_Q, the new set of scaled potentials is now written in the general form

$$V_D(\mathbf{R}) = \lambda_D^{(1)} V_D^{(1)} + \sum_{i=1}^{3} \lambda_{D,i}^{(2)} V_{D,i}^{(2)}(R_i) + \lambda_D^{(3)} V_D^{(3)}(\mathbf{R}) \tag{2}$$

$$V_Q(\mathbf{R}) = \lambda_Q^{(1)} V_Q^{(1)} + \sum_{i=1}^{3} \lambda_{Q,i}^{(2)} V_{Q,i}^{(2)}(R_i) + \lambda_Q^{(3)} V_Q^{(3)}(\mathbf{R}) \tag{3}$$

where $\lambda_{D,i}^{(n)}$ and $\lambda_{Q,i}^{(n)}$ are multiplicative constants to ensure that the various n-atom species in the cluster expansion reproduce the experimental atomic excitation energy ($n = 1$) or the dissociation energy ($n \geq 2$) values; a single one-body term has been assumed for simplicity; see elsewhere.[39] If the scaling were applied only to the dynamical correlation part of the ab initio energy, one would be led to the DMBE-SEC[6] (DMBE with scaling of the external correlation) method, but it would require a refit of the full potential. Indeed, the dynamical correlation is known to have a physical origin and hence is largely scaleable, while the EHF energy is system-specific and less prone to scaling (perhaps even more so in DMBE for the reasons given above). However, this may not be a severe limitation if scaling of the EHF energy is moderate and mostly limited to specific regions of the PES, namely, near-equilibrium geometries of the various n-body fragments. In fact, the EHF energy is known to vanish exponentially with one or more interatomic distances and hence not bring significant concern away from the scaling point, in particular, along the asympototic channels. It is this assumption that will be tested in the current work by scaling the total energy of the fitted n-body terms in the DMBE form (DMBE-STE). We emphasize that the DMBE-SEC[6] method should not be used here because the dc term of the DMBE potentials contains long-range contributions[22,24,25] other than the dynamical correlation.

Given the symmetry of the title species, all n-body scaling factors must be identical. Thus, the scaled DMBE-STE potentials assume here the form

$$V_D(\mathbf{R}) = \lambda_D^{(1)} V_D^{(1)} + \lambda_D \sum_{i=1}^{3} V_D^{(2)}(R_i) + \lambda_D V_D^{(3)}(\mathbf{R}) \tag{4}$$

$$V_Q(\mathbf{R}) = \lambda_Q^{(1)} V_Q^{(1)} + \lambda_Q \sum_{i=1}^{3} V_Q^{(2)}(R_i) + \lambda_Q V_Q^{(3)}(\mathbf{R}) \tag{5}$$

with the scaling parameters being $\lambda_D = \lambda_{D,i}^{(2)}$ and $\lambda_Q = \lambda_{Q,i}^{(2)}$, $\forall i$, one per electronic state. Of course, $\lambda^{(n\geq 3)}$ can be chosen distinctly to fit some data on the n-atom system, but we keep the formalism here at its simplest level. In fact, there is an estimate of the dissociation energy for doublet N_3, but the error is[14] 2.4 kcal mol^{-1}. Additionally, for heteronuclear systems, it is likely (by analogy with what is commonly done in DMBE-SEC) that $\lambda^{(n\geq 3)}$ can be well represented by the average of the two-body $\lambda_D^{(2)}$ scaling factors. One gets $\lambda_D = 1.048653$ and $\lambda_Q = 1.006293$ from the requirement that both diatomic potentials match the experimental dissociation energy[40] at equilibrium. The STE-scaled two-body terms are shown in Figure 2 together with the original forms. Although the STE curve for the quartet state lies close, as expected, to the CBS one, this is not at all true for the doublet that was fitted to AVTZ energies. Note that $\lambda_D^{(1)} = 0.969147$ such as to warrant that the doublet and quartet PESs are correctly separated by the $N(^2D) - N(^4S)$

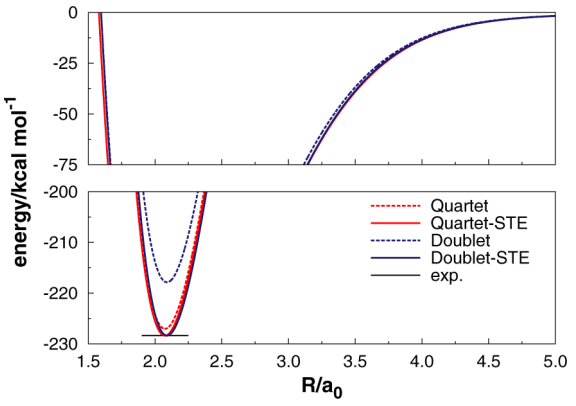

Figure 2. N_2: the STE curves are chosen to mimic the experimental dissociation energy.[40]

dx.doi.org/10.1021/jp5087027 | J. Phys. Chem. A 2014, 118, 10127−10133

experimental gap.[41] The value of $\lambda_Q^{(1)}$ is immaterial because the $N(^4S) + N_2$ asymptote is chosen as the reference energy for the whole set of PESs. Note further that the above formalism has assumed a single-sheeted adiabatic potential, although it applies identically to the various diabatic sheets of a matrix potential,[22,23,26] this being actually the case for the azide $^2A'$ doublet states here examined.

PROPERTIES OF THE DMBE-STE POTENTIALS

Figures 3 and 4 show contour plots of attributes of the quartet and doublet PESs of azide. While Figure 3 aims to

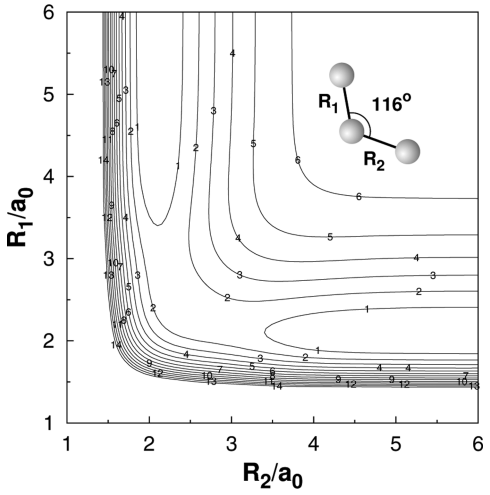

Figure 3. Contour plot of the energy difference between the DMBE-STE and DMBE PESs for N_3 bond stretching, with the bond angle fixed at 116 °. Contours start at number 0, with the counter increasing uniformly with an associated energy spacing of +0.2 kcal mol^{-1}.

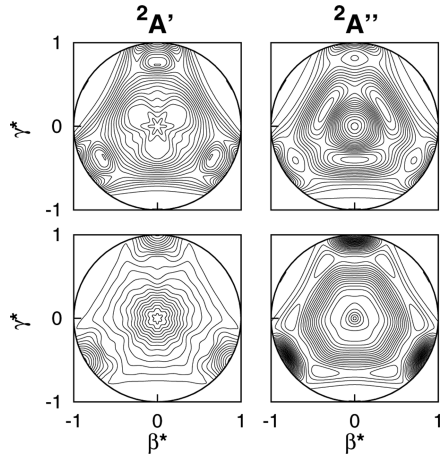

Figure 4. Optimized relaxed triangular plots in hyperspherical coordiantes[42] for the doublet-state DMBE-STE potentials of N_3. Top panels refer to the ground state of each symmetry and bottom ones to the excited states. Contours and energy spacing as those elsewhere.[28,29]

quantitatively show the differences between the DMBE fit to CBS data[27] and the DMBE-STE potential here reported, Figure 4 pinpoints topographical features of the doublet DMBE-STE forms, which are shown to remain essentially unaltered when compared to the DMBE fits[28,29] of the raw MRCI/AVTZ data.

Tables 1−3 gather the geometric and energetic (relative to the appropriate asymptotes) attributes of the various stationary

Table 1. Stationary Points of the $N_3(^4A'')$ PES at CCSD(T)/AVTZ and CBS/CCSD(T)

		CCSD(T)		fitted	
feature	feature	AVTZ	CBS	DMBE	DMBE-STE
min[b] (C_{2v})	r_1/a_0	2.39	2.38	2.38	2.38
	r_2/a_0	2.39	2.38	2.38	2.38
	Θ/deg	119	119	119	119
	ΔE^a	44.7	42.9	42.9	43.1
sp (C_s)	r_1/a_0	2.22	2.20	2.20	2.20
	r_2/a_0	2.84	2.85	2.83	2.83
	Θ/ deg	117	117	116	116
	ΔE^a	47.1	45.9	45.9	46.2

[a]In kcal mol^{-1}, relative to the $N(^4S) + N_2$ asymptote. [b]Volcano-like minimum between the two permutationally equivalent C_s saddle points.[27]

Table 2. Stationary Structures of $N_3(1^2A'')$[a]

		MRCI(Q)			fitted	
structure	feature	AVTZ[b]	AVQZ[c]	CBS[c]	DMBE	DMBE-STE
$^2\Pi_g$	R/a_0	2.24			2.24	2.24
	θ/deg	180			180	2.24
	ΔV	0.0	0.0	0.0	0.0	0.0
cyc-N_3	R/a_0	2.77			2.77	2.76
	θ/deg	49.8			50.0	50.0
	ΔV	32.2	32.9	33.3	32.3	33.8
TS_{pseudo}	R/a_0	2.47			2.47	2.47
	θ/deg	71.9			71.8	71.8
	ΔV	33.1	33.7	34.1	33.2	34.8
MSX	R/a_0	2.59			2.59	2.59
	θ/deg	60.0			60.0	60.0
	ΔV	45.4			45.0	47.2
$TS_{isom}^{C_s}$	R_1/a_0	2.31			2.26	2.26
	R_2/a_0	2.62			2.70	2.70
	θ/deg	109			109	109
	ΔV	65.0	66.4	67.4	65.1	68.3
$TS_{diss}^{C_{\infty v}}$	R_1/a_0	4.23			4.19	4.19
	R_2/a_0	2.09			2.09	2.09
	θ/deg	180			180	180
	ΔV	61.8	63.2	64.2	61.8	64.7
$TS_{diss}^{C_{2v}}$	R/a_0	4.23			4.16	4.16
	θ/deg	28.9			29.4	29.4
	ΔV	65.7	67.3	68.3	65.8	69.0
$N(^2D) + N_2$	ΔV	59.0	60.4	61.4	59.0	61.9

[a]Energies are in kcal mol^{-1} relative to the ground $\tilde{X}^2\Pi_g$ state. [b]From ref 43. [c]At the geometries of column 3.

points (labeled as those elsewhere[27−29]), which show a remarkable agreement with the CBS data. As expected, the changes for the quartet state are seen to be minor because the fitted raw energies were already at the CBS level. In fact, the energetic differences for the $1^4A'$ state reach at most 0.3 kcal mol^{-1} for the two stationary structures, and their geometries are not visibly changed. In turn, for the $N_3(1^2A'')$ state, the DMBE-STE structures lie remarkably closer to the ab initio CBS values than the DMBE ones; the differences are typically around 0.5 kcal mol^{-1} and reach at most 0.9 kcal mol^{-1}. Note that the scaling is supposed to account for CBS and beyond (core correlation, truncation of the $\mathcal{N}$-electron expansion, non-adiabaticity, and so on), and therefore, it is hard to say which of the CBS and DMBE-STE values is more realistic. Clearly, the

dx.doi.org/10.1021/jp5087027 | J. Phys. Chem. A 2014, 118, 10127−10133

Table 3. Stationary Structures of $N_3(2^2A'')$[a]

		MRCI(Q)			fitted	
feature	feature	AVTZ[b]	AVQZ[c]	CBS[c]	DMBE	DMBE-STE
$^2\Pi_u$	R/a_0	2.41			2.40	2.40
	θ/deg	180			2.40	2.40
	ΔV	104	106	107	105	110
min_{B_1}	R/a_0	2.39			2.38	2.38
	θ/deg	120			122	122
	ΔV	72.8	73.5	74.0	72.9	76.5
TS_{B_1}	R/a_0	2.57			2.55	2.55
	θ/deg	86.1			85.3	85.3
	ΔV	109	111	112	108	113.4
TS_{C_s}	R_1/a_0				3.04	3.04
	R_2/a_0				2.17	2.17
	θ/deg				119	119
	ΔV				79.8	83.6

[a]Energies are in kcal mol^{-1} relative to the ground $\tilde{X}^2\Pi_g$ state. [b]From ref 44. [c]At the geometries of column 3.

geometrical attributes show also changes of minor concern with respect to the original DMBE form. In somewhat less good agreement, the energetic differences in the excited $2^2A''$ state attain 3.0 kcal mol^{-1}. Interestingly, except for the quartet PES where the barrier is slightly larger, both doublet states tend to show DMBE-STE attributes slightly more attractive than the corresponding CBS values, possibly because the latter account only for the extrapolation to the CBS limit. Furthermore, Figure 5 shows that the good agreement extends to the

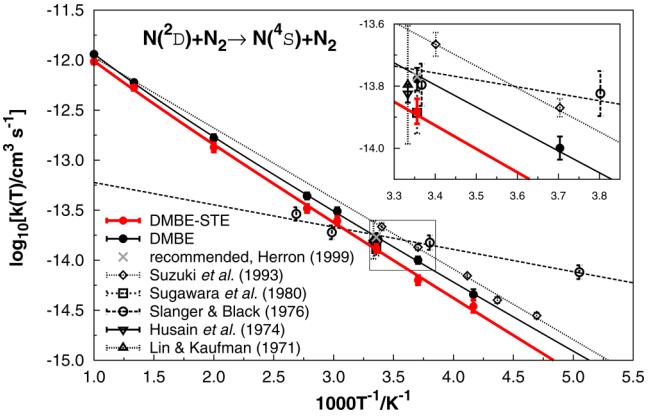

Figure 5. Harmonic frequencies of stationary structures for the lowest $^2A''$ state of N_3. The pink bars refer to the original DMBE PES and the blue ones to DMBE-STE. The three modes are plotted on top of each other (including imaginary ones); thus, the heigher the bar, the higher the vibrational frequency. Energies on te x-axis are relative to the $N(^2D) + N_2$ limit.

vibrational harmonic frequencies, with a consistent increase of 2.4% for all modes (the numerical frequencies and a more complete version of Table 2 are given as Supporting Information (SI)). This stems from the constant scaling (λ_D = 1.048653) of the PES, with the frequencies (which are proportional to the square root of the eigenvalues of the Hessian matrix) being then scaled by $(\lambda_D)^{1/2}$ = 1.024. It also implies that the DMBE-STE forms largely maintain parallelity to the DMBE ones, a key requirement for dynamics studies.

EXCHANGE AND ELECTRONIC QUENCHING IN N + N_2 COLLISIONS

Trajectories were run on the DMBE-STE forms here reported for the quartet (Q) and doublet (D) states of the N_3 radical by using the quasiclassical trajectory (QCT[45,46]) method, an approach well justified due to the large masses involved.[37] Using only the Q-state PES, rate constants were calculated for the exchange reaction $N(^4S) + N_2 \rightarrow N_2 + N(^4S)$, which is part of a set of reactions that occur under extreme environmental conditions such as the ones that happen when objects enter the Earth's atmosphere, and hence, it is relevant for the designing of heat shields for space vehicles.[47] Note that our formerly reported DMBE PES has yielded reliable results for temperature regimes where experiments cannot be conducted, and here, we show that the rate constants calculated from the DMBE-STE Q-state form essentially reproduce our previous results. Note further that the dynamics study here conducted follows the same methodology as that described in ref 37. Briefly, the reactants are initially separated by 9 Å and the initial rovibrational state of the diatomic selected from its probability distribution, with the rovibrational levels calculated by solving the nuclear Schrödinger equation for the diatomic fragment[48] of the DMBE-STE PES here reported. Given that the barrier for this reaction is high, the probability of finding a trajectory above the classical threshold for reaction is very low. For example, at T = 1273 K, only about 2 in 10^7 trajectories have sufficient translational energy to overcome the barrier. To speed up the calculations, we have developed an important sampling method for the translational energy[37] by sectioning its Boltzmann distribution, thus allowing a different number of trajectories to be run for each sector according to the desired statistics (for further details, see ref 37). The quantum mechanical threshold[49] scheme has also been employed here, which saves computational time by integrating only trajectories with total energy above the barrier. The results are compared in Table 4 with the ones obtained from the DMBE[37] and other[47,50] PESs. As could be anticipated, they are hardly distinguishable from the DMBE ones.[37]

Calculations on the DMBE-STE forms for the D and Q states were also performed for the electronic quenching reaction $N(^2D) + N_2 \rightarrow N(^4S) + N_2$ by following the procedure described elsewhere;[32] electronic transitions were allowed via trajectory surface hopping[54−56] (TSH) in a way similar to that suggested by Marks and Thompson.[57] Succintly, the trajectories are interrogated at every integration step whether a D/Q crossing of the PESs has occurred, in which case the integration goes back one step and continues with a 200× smaller time step such as to locate precisely the point

Table 4. Logarithm of the Thermal Rate Coefficients (in cm^{3}s^{-1}) for the $N(^4S) + N_2$ Exchange Reaction

T (K)	DMBE[a]	DMBE-STE[a]	L4[a]	WSHDSP[b]	exp.
1273	−18.27 ± 0.04	−18.34	−18.54	−18.5	≤−16.9[c]
3400	−12.87 ± 0.02	−12.88	−12.99	−13.0	−12.3 ± 1.0[d]

[a]QCT calculations. [b]Reference 51. [c]Reference 52. [d]Reference 53.

dx.doi.org/10.1021/jp5087027 | J. Phys. Chem. A 2014, 118, 10127−10133

where the Landau–Zener transition probability for diabatic crossing is calculated[57,58]

$$P_{LZ} = 1 - \exp\left(\frac{-2\pi V_{SO}^2}{\hbar|\Delta F v|}\right) \quad (6)$$

where ΔF is the difference in forces at the two surfaces and v the velocity, both calculated at the crossing point and orthogonally to the seam. As before,[32] the spin–orbit coupling V_{SO} is taken from ref 43 and deemed to be representative of the most relevant crossing regions. Additionally, the $2A'$ and $^2A''$ PESs are assumed as decoupled[32] because after hopping to the quartet state, the system experiences a strong gradient toward dissociation. Thus, the total cross section assumes the form

$$\sigma = \sigma_{^2A' \rightarrow {}^4A''} + \sigma_{^2A'' \rightarrow {}^4A''} \quad (7)$$

with the calculated rate constants and associated 68% error bars shown in Figure 6, jointly with the results from the DMBE PES

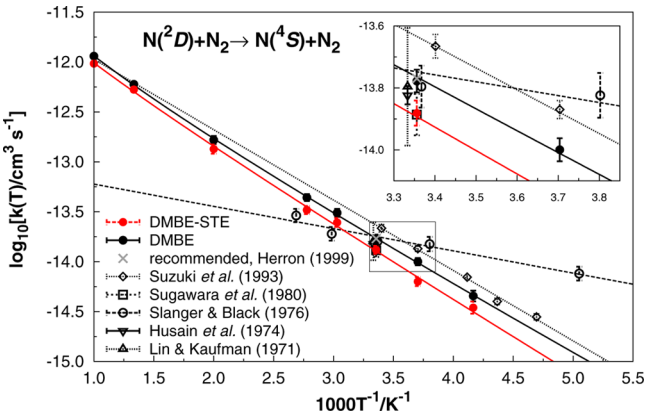

Figure 6. Comparison of calculated rate constants for the reaction $N(^2D) + N_2 \rightarrow N(^4S) + N_2$ (from DMBE[32] and DMBE-STE) with experimental[59−63] and recommended[64] data.

and experimental data. Clearly, the agreement with the values[32] from DMBE is very good, with no further remarks due on the comparison with experiment. Suffice it to add that the calculated rate constant is now slightly smaller, possibly due to the larger barrier for the $N(^2D) + N_2$ reaction in DMBE-STE [0.13 kcal mol^{-1}; hence, ∼5% larger than that in DMBE (2.8 kcal mol^{-1})]. The agreement is now best with the experimental datum of Sugawara et al.[60] but still excellent with the recommended[64] value at 300 K. Indeed, the current result and the one previously reported will possibly delimit a most "likely range" for the rate of electronic quenching in $N(^2D) + N_2$ collisions.

CONCLUDING REMARKS

We have suggested a simple pragmatic procedure to bring an ab-initio-based PES into consistency with experimental data that is known to play a key role in reaction dynamics. The scheme uses a minimum of empirical information and is expected to introduce no artifactual changes. Thus, it can be extremely useful in cases where the raw data used to calibrate the PES are trustworthy but not sufficiently quantitative, as is the case when a small one- or N-electron basis (or both) is employed. Although applied here to a set of homonuclear systems, there is no reason in principle to believe that it may not work otherwise. Such a belief stems from the method itself, which uses one of the major assets of writing the PES as a MBE of the total molecular potential energy. As a result, the present scheme is expected to be also applicable to larger polyatomic situations.

ASSOCIATED CONTENT

Supporting Information

The values of the harmonic frequencies for the $^2A''$ potential energy surface and a more complete version of Table 2 are given. This material is available free of charge via the Internet at http://pubs.acs.org.

AUTHOR INFORMATION

Corresponding Authors

*E-mail: varandas@uc.pt (A.J.C.V.).
*E-mail: brenogalvao@gmail.com (B.R.L.G.).

Notes

The authors declare no competing financial interest.

ACKNOWLEDGMENTS

This work has the support of Fundação para a Ciência e a Tecnologia, Portugal (Contracts PTDC/CEQ-COM3249/2012 and PTDC/AAG-MAA/4657/2012). Support of the Coimbra Chemistry Centre (Project PEst-OE/QUI/UI0313/2014) and Conselho Nacional de Desenvolvimento Científico e Tecnológico (Brazil) is also gratefully acknowledged.

REFERENCES

(1) Helgaker, T.; Klopper, W.; Koch, H.; Noga, J. Basis-Set Convergence of Correlated Calculations on Water. *J. Chem. Phys.* **1997**, *106*, 9639–9646.
(2) Varandas, A. J. C. Extrapolating to the One-Electron Basis-Set Limit in Electronic Structure Calculations. *J. Chem. Phys.* **2007**, *126*, 244105.
(3) Brown, F. B.; Truhlar, D. G. A New Semi-Empirical Method of Correcting Large-Scale Configuration Interaction Calculations for Incomplete Dynamic Correlation of Electrons. *Chem. Phys. Lett.* **1985**, *117*, 307–313.
(4) Gordon, M. S.; Truhlar, D. G. Scaling All Correlation Energy in Perturbation Theory Calculations of Bond Energies and Barrier Heights. *J. Am. Chem. Soc.* **1986**, *108*, 5412–5419.
(5) Gordon, M. S.; Nguyen, K. A.; Truhlar, D. G. Parameters for Scaling the Correlation Energy of the Bonds Si–H, P–H, S–H, and Cl–Hand Application to the Reaction of Silyl Radical with Silane. *J. Phys. Chem.* **1989**, *93*, 7356–7358.
(6) Varandas, A. J. C. A Semiempirical Method for Correcting Configuration Interaction Potential Energy Surfaces. *J. Chem. Phys.* **1989**, *90*, 4379–4391.
(7) Murrell, J. N.; Carter, S.; Farantos, S. C.; Huxley, P.; Varandas, A. J. C. *Molecular Potential Energy Functions*; Wiley: Chichester, U.K., 1984.
(8) Sorbie, K. S.; Murrell, J. N. Analytical Potentials for Triatomic Molecules from Spectroscopic Data. *Mol. Phys.* **1975**, *29*, 1387–1407.
(9) Murrell, J. N.; Sorbie, K. S.; Varandas, A. J. C. Analytical Potential of Triatomic Molecules from Spectroscopic Data II. Application to Ozone. *Mol. Phys.* **1976**, *32*, 1359–1372.
(10) Thrush, B. A. The Detection of Free Radicals in the High Intensity Photolysis of Hydrogen Azide. *Proc. R. Soc. London, Ser. A* **1956**, *235*, 143–147.
(11) Douglas, A. E.; Jones, W. J. The 2700 Å Bands of N_3. *Can. J. Phys.* **1965**, *43*, 2216–2221.
(12) Beaman, R. A.; Nelson, T.; Richards, D. S.; Setser, D. W. Observation of N_3 by Laser-Induced Fluorescence. *J. Phys. Chem.* **1987**, *91*, 6090–6092.
(13) Brazier, C. R.; Bernath, P. F.; Burkholder, J. B.; Howard, C. J. Fourier Transform Spectroscopy of the ν_3 Band of the N_3 Radical. *J. Chem. Phys.* **1988**, *89*, 1762–1767.

(14) Continetti, R. E.; Cyr, D. R.; Osborn, D. L.; Leahy, D. J.; Neumark, D. M. Photodissociation Dynamics of the N_3 Radical. *J. Chem. Phys.* **1993**, *99*, 2616−2631.
(15) Hansen, N.; Wodtke, A. M. Velocity Map Ion Imaging of Chlorine Azide Photolysis: Evidence for Photolytic Production of Cyclic-N_3. *J. Phys. Chem. A* **2003**, *107*, 10608−10614.
(16) Samartzis, P. C.; J. J.-M. Lin, T.-T. C.; Chaudhuri, C.; Lee, Y. T.; Lee, S.-H.; Wodtke, A. M. Two Photoionization Thresholds of N_3 Produced by ClN_3 Photodissociation at 248 nm: Further Evidence for Cyclic N_3. *J. Chem. Phys.* **2005**, *123*, 051101.
(17) Zhang, J.; Zhang, P.; Chen, Y.; Yuan, K.; Harich, S. A.; Wang, X.; Wang, Z.; Yang, X.; Morokuma, K.; Wodtke, A. M. An Experimental and Theoretical Study of Ring Closing Dynamics in HN_3. *Phys. Chem. Chem. Phys.* **2006**, *8*, 1690−1696.
(18) Samartzis, P. C.; J. J.-M. Lin, T.-T. C.; Chaudhuri, C.; Lee, S.-H.; Wodtke, A. M. The Simplest All-Nitrogen Ring: Photolytically Filling the Cyclic-N_3 Well. *J. Chem. Phys.* **2007**, *126*, 041101.
(19) Samartzis, P. C.; Wodtke, A. M. Casting a New Light on Azide Photochemistry: Photolytic Production of Cyclic-N_3. *Phys. Chem. Chem. Phys.* **2007**, *9*, 3054−3066.
(20) Larson, C.; Ji, Y.; Samartzis, P. C.; Quinto-Hernandez, A.; Lin, J. J.; Ching, T.-T.; Chaudhuri, C.; Lee, S.-H.; Wodtke, A. M. Observation of Photochemical C−N Bond Cleavage in CH_3N_3: A New Photochemical Route to Cyclic N_3. *J. Phys. Chem. A* **2008**, *112*, 1105−1111.
(21) Eyring, H.; Polanyi, M. Concerning Simple Gas Reactions. *Z. Phys. Chem. B* **1931**, *12*, 279−331.
(22) Varandas, A. J. C. In *Conical Intersections: Electronic Structure, Dynamics & Spectroscopy*; Domcke, W., Yarkony, D. R., Köppel, H., Eds.; Advanced Series in Physical Chemistry; World Scientific Publishing: River Edge, NJ, 2004; Vol. *15*; Chapter 5, p 205.
(23) Varandas, A. J. C. In *Reaction Rate Constant Computations: Theories and Applications*; Han, K., Chu, T., Eds.; The Royal Society of Chemistry: London, 2014; Vol. *17*; Chapter Putting together the pieces: global description of valence and long-range forces via combined hyperbolic inverse-power representation of the potential energy surface for use in reaction dynamics, pp 408−445.
(24) Varandas, A. J. C. A Double Many-Body Expansion of Molecular Potential Energy Functions. I. Hartree−Fock-Approximate Correlation Energy (HFACE) Potential for the Helium−Hydrogen (HeH_2) van der Waals Molecule. *Mol. Phys.* **1984**, *53*, 1303−1325.
(25) Varandas, A. J. C. Intermolecular and Intramolecular Potentials: Topographical Aspects, Calculation, and Functional Representation via a DMBE Expansion Method. *Adv. Chem. Phys.* **1988**, *74*, 255−338.
(26) Varandas, A. J. C. Combined-Hyperbolic-Inverse-Power-Representation of Potential Energy Surfaces: A Preliminary Assessment for H_3 and HO_2. *J. Chem. Phys.* **2013**, *138*, 054120.
(27) Galvão, B. R. L.; Varandas, A. J. C. Accurate Double Many-Body Expansion Potential Energy Surface for N_3 from Correlation Scaled Ab Initio Energies with Extrapolation to the Complete Basis Set Limit. *J. Phys. Chem. A* **2009**, *113*, 14424−14430.
(28) Galvão, B. R. L.; Varandas, A. J. C. Ab Initio Based Double-Sheeted DMBE Potential Energy Surface for $N_3(^2A'')$ and Exploratory Dynamics Calculations. *J. Phys. Chem. A* **2011**, *115*, 12390−12398.
(29) Galvão, B. R. L.; Caridade, P. J. S. B.; Varandas, A. J. C. $N(^4S/^2D)+N_2$: Accurate Ab Initio-Based DMBE Potential Energy Surfaces and Surface-Hopping Dynamics. *J. Chem. Phys.* **2012**, *137*, 22A515.
(30) Varandas, A. J. C.; Piecuch, P. Extrapolating Potential Energy Surfaces by Scaling Electron Correlation at a Single Geometry. *Chem. Phys. Lett.* **2006**, *430*, 448−453.
(31) Varandas, A. J. C. Accurate Global Ab Initio Potentials at Low-Cost by Correlation Scaling and Extrapolation to the One-Electron Basis Set Limit. *Chem. Phys. Lett.* **2007**, *443*, 398−407.
(32) Galvão, B. R. L.; Varandas, A. J. C.; Braga, J. P.; Belchior, J. C. Electronic Quenching of $N(^2D)$ by N_2: Theoretical Predictions, Comparison with Experimental Rate Constants, and Impact on Atmospheric Modeling. *J. Phys. Chem. Lett.* **2013**, *4*, 2292−2297.
(33) Esposito, F.; Capitelli, M. QCT Calculations for the Process $N_2(v)+N \rightarrow N_2(v')+N$ in the Whole Vibrational Range. *Chem. Phys. Lett.* **2006**, *418*, 581−585.
(34) Esposito, F.; Capitelli, M. Quasiclassical Molecular Dynamic Calculations of Vibrationally and Rotationally State Selected Dissociation Cross-Sections: $N + N_2(v,j) \rightarrow 3N$. *Chem. Phys. Lett.* **1999**, *302*, 49.
(35) Capitelli, M.; Colonna, G.; D'Ammando, G.; Laporta, V.; Laricchiuta, A. Nonequilibrium Dissociation Mechanisms in Low Temperature Nitrogen and Carbon Monoxide Plasmas. *Chem. Phys.* **2014**, *438*, 31−36.
(36) Munafò, A.; Magin, T. E. Modeling of Stagnation-Line Nonequilibrium Flows by Means of Quantum Based Collisional Models. *Phys. Fluids* **2014**, *26*, 097102.
(37) Caridade, P. J. S. B.; Galvão, B. R. L.; Varandas, A. J. C. Quasiclassical Trajectory Study of Atom-Exchange and Vibrational Relaxation Processes in Collisions of Atomic and Molecular Nitrogen. *J. Phys. Chem. A* **2010**, *114*, 6063−6070.
(38) Galvão, B. R. L.; Varandas, A. J. C.; Braga, J. P.; Belchior, J. C. Electronic Quenching in $N(^2D) + N_2$ Collisions: A State-Specific Analysis via Surface Hopping Dynamics. *J. Chem. Theory Comput.* **2014**, *10*, 1872−1877.
(39) Li, J.; Varandas, A. J. C. Accurate Double Many-Body Expansion Potential Energy Surface for the 2^1A State of N_2O. *J. Chem. Phys.* **2014**, *141*, 084307.
(40) Herzberg, G. *Molecular Spectra and Molecular Structure. I. Spectra of Diatomic Molecules*, 2nd ed.; Van Nostrand: New York, 1950.
(41) Kramida, A.; Yu, R.; Reader, J.; NIST ASD Team. *NIST Atomic Spectra Database*, version 5.1. National Institute of Standards and Technology, Gaithersburg, MD; http://physics.nist.gov/asd (Aug 1, 2013).
(42) Varandas, A. J. C. A Useful Triangular Plot of Triatomic Potential Energy Surfaces. *Chem. Phys. Lett.* **1987**, *138*, 455−461.
(43) Zhang, P.; Morokuma, K.; Wodtke, A. M. High-Level Ab Initio Studies of Unimolecular Dissociation of the Ground-State N_3 Radical. *J. Chem. Phys.* **2005**, *122*, 014106.
(44) Wang, Z.; Kerkines, I. S. K.; Morokuma, K.; Zhang, P. Analytical Potential Energy Surfaces for N_3 Low-Lying Doublet States. *J. Chem. Phys.* **2009**, *130*, 044313.
(45) Hase, W. L.; Duchovic, R. J.; Hu, X.; Komornicki, A.; Lim, K. F.; Lu, D.; Peslherbe, G. H.; Swamy, K. N.; Linde, S. R. V.; Varandas, A. J. C.; et al. VENUS96: A General Chemical Dynamics Computer Program. *QCPE Bull.* **1996**, *16*, 43.
(46) Peslherbe, G. H.; Wang, H.; Hase, W. L. Monte Carlo Sampling for Classical Trajectory Simulations. *Adv. Chem. Phys.* **1999**, *105*, 171−201.
(47) Wang, D.; Stallcop, J. R.; Huo, W. M.; Dateo, C. E.; Schwenke, D. W.; Partridge, H. Quantal Study of the Exchange Reaction for N + N_2 Using an Ab Initio Potential Energy Surface. *J. Chem. Phys.* **2003**, *118*, 2186−2189.
(48) LeRoy, R. J. *LEVEL 7.5*, A computer program for Solving the Radial Schrödinger Equation for Bound and Quasi-bound Levels, University of Waterloo Chemical Physics Research Report CP-655; University of Waterloo: Ontario, Canada, 2002.
(49) Truhlar, D. G. Accuracy of Trajectory Calculations and Transition State Theory for Thermal Rate Constants of Atom Transfer Reactions. *J. Chem. Phys.* **1979**, *83*, 188−199.
(50) Garcia, E.; Saracibar, A.; Gomez-Carrasco, S.; Laganà, A. Modeling the Global PES of the $N+N_2$ Reaction from Ab Initio Data. *Phys. Chem. Chem. Phys.* **2008**, *10*, 2552−2558.
(51) Garcia, E.; Saracibar, A.; Laganà, A.; Skouteris, D. The Shape of the Potential Energy Surface and the Thermal Rate Coefficients of the N + N_2 Reaction. *J. Phys. Chem. A* **2007**, *111*, 10362−10368.
(52) Bar-Nun, A.; Lifshitz, A. Kinects of the Homogeneous Exchange Reaction $^{14-14}N_2 + {}^{15-15}N_2 \rightarrow 2\,{}^{14-15}N_2$. Single-Pulse Shock Tube Studies. *J. Chem. Phys.* **1967**, *47*, 2878−2888.
(53) Lyon, R. K. Search for the N−N_2 Exchange Reaction. *Can. J. Chem.* **1972**, *50*, 1437−1440.

(54) Tully, J. C.; Preston, R. K. Trajectory Surface Hopping Approach to Nonadiabatic Molecular Collisions: The Reaction of H^+ with D_2. *J. Chem. Phys.* **1971**, *55*, 562−572.
(55) Zahr, G. E.; Preston, R. K.; Miller, W. H. Theoretical Treatment of Quenching in $O(^1D)$ + N_2 Collisions. *J. Chem. Phys.* **1975**, *62*, 1127−1135.
(56) Voronin, A. I.; Marques, J. M. C.; Varandas, A. J. C. Trajectory Surface Hopping Study of the Li + $Li_2(X^1\Sigma_g^+)$ Dissociation Reaction. *J. Phys. Chem. A* **1998**, *102*, 6057−6062.
(57) Marks, A. J.; Thompson, D. L. A Trajectory Surface-Hopping Study of Mode Specificity in the Predissociation of N_2O. *J. Chem. Phys.* **1991**, *95*, 8056−8064.
(58) Tachikawa, H.; Hamabayashi, T.; Yoshida, H. Electronic-to-Vibrational and -Rotational Energy Transfer in the $O(^1D)$+N_2 Quenching Reaction: Ab Initio MO and Surface-Hopping Trajectory Studies. *J. Chem. Phys.* **1995**, *99*, 16630−16635.
(59) Suzuki, T.; Shihira, Y.; Sato, T.; Umemoto, H.; Tsunashima, S. Reactions of $N(^2D)$ and $N(^2P)$ with H_2 and D_2. *J. Chem. Soc., Faraday Trans.* **1993**, *89*, 995−999.
(60) Sugawara, K.; Ishikawa, Y.; Sato, S. The Rate Constants of the Reactions of the Metastable Nitrogen-Atoms, ^2D and ^2P, and the Reactions of $N(^4S)$+NO → N_2 + $O(^3P)$ and $O(^3P)$ + NO + M → NO_2 + M. *Bull. Chem. Soc. Jpn.* **1980**, *53*, 3159−3164.
(61) Slanger, T. G.; Black, G. Quenching of $N(^2D)$ by N_2 and H_2O. *J. Chem. Phys.* **1976**, *64*, 4442−4444.
(62) Husain, D.; Mitra, S. K.; Young, A. N. Kinetic Study of Electronically Excited Nitrogen Atoms, $N(2^2D_J,2^2P_J)$, by Attenuation of Atomic Resonance Radiation in the Vacuum Ultra-violet. *J. Chem. Soc., Faraday Trans.* **1974**, *70*, 1721−1731.
(63) Lin, C.-L.; Kaufman, F. Reactions of Metastable Nitrogen Atoms. *J. Chem. Phys.* **1971**, *55*, 3760−3770.
(64) Herron, J. T. Evaluated Chemical Kinetics Data for Reactions of $N(^2D)$, $N(^2P)$, and $N_2(A^3\Sigma_u^+)$ in the Gas Phase. *J. Phys. Chem. Ref. Data* **1999**, *28*, 1453−1483.